Surface/Interface-Related Conductivity in Nanometer Thick YSZ Films

Igor Kosacki,[a,z] **Christopher M. Rouleau,**[b] **Paul F. Becher,**[a] **James Bentley,**[a] **and Douglas H. Lowndes**[b]

Oak Ridge National Laboratory, [a]Metals and Ceramics Division and [b]Condensed Matter Sciences Division, Oak Ridge, Tennessee 37831, USA

Results of the electrical conductivity study of highly textured, ultrathin (15 nm) cubic yttria-stabilized zirconia (YSZ) thin films are presented for the first time. A nanoscale effect that results in exceptionally high ionic conductivity at moderate temperatures is detected in films less than 60 nm thick. The conductivity increases continuously below this level and reaches 0.6 S/cm at 800°C for a 15 nm thick film, which represents the highest reported value for the YSZ system. The observed behavior is attributed to an increasingly significant contribution of the surface/interface conductivity with decreasing film thickness. These observations can have important implications for the development of nanostructured electrochemical devices with enhanced performance.
© 2004 The Electrochemical Society. [DOI: 10.1149/1.1809556] All rights reserved.

The development of materials with enhanced ionic conductivity and catalytic properties is of prime importance for devices based on electrochemical reactions (*e.g.*, fuel cells, batteries, and ionic membranes). Ionic transport has generally been increased in oxide electrolytes (*e.g.*, ZrO_2 and CeO_2) by the generation of mobile oxygen vacancies, which are created by acceptor doping. However, there is an optimum doping level, typically 15-20 atom % due to the diffusivity limited by lattice distances for hopping ions.[1-3] Based on the lattice diffusion model, the maximum value of ionic conductivity for acceptor-doped ZrO_2 was estimated to be ~10 S/cm, which can only be achieved near the melting point, where the activation energy is reduced to zero.[4] To significantly enhance the ionic conductivity, it is necessary to accentuate rapid transport mechanisms. This appears to be possible when the material microstructure is in the nanometer range due to the dominant role of the grain boundary and surface effects, which can exhibit orders of magnitude greater diffusivity than the lattice. Recent studies have discussed the enhanced conductivity of nanocrystalline CeO_2 and ZrO_2:(Y- or Sc-doped) thin films.[5-9] For example, a fifty-fold increase in the ionic conductivity has been observed in 20 nm grain-sized YSZ thin films as compared to that of conventional microcrystalline ceramics or single crystals.[5,8] Such enhancement can be attributed to either the greatly reduced impurity concentration at grain boundaries[10] or the dominance of size-dependent defect equilibria[5,11] as the grain size is reduced below 100 nm. The ionic conductivity of YSZ can also be enhanced by the introduction of a high density of dislocations,[12] which act as rapid diffusion paths for oxygen vacancies (*e.g.*, pipe diffusion[13]).

The termination of an ionic material by a surface or interface creates a space-charge region within which the concentration of defects is different from that of the bulk region and can affect the increasing of the conductivity. Such an idea has been discussed for CaF_2 nanocrystalline specimens[14] and more recent for BaF_2/CaF_2 super lattices, where the substantial increase of ionic conductivity was observed.[15] The point that still eludes researchers is whether the observed enhancements of the ionic conductivity in nanocrystalline materials are attributed to enhanced mobility, to changes in the defect equilibria, or to an increased contribution of space-charge effects.

The studies mentioned above were performed on ceramic materials where the negative effects of blocking grain boundaries can influenced the electrical transport. These can be minimized when epitaxial solid electrolyte thin films are used. In such system, a single interface can provide very rapid transport with the absence of any grain boundary blocking contribution. The approach taken here is to characterize the in-plane temperature-dependent conductivity

of highly textured YSZ films. The objective of this study was to determine the conditions where the surface/interface effects dominate the bulk properties. Nanoscale effects can influence the conductivity when the film thickness reaches values where the combined interface and surface regions become a significant fraction of the film thickness. This effect should vary with the film thickness. The objective of this study was to determine the electrical conductivity related to surface/interface effects in highly textured cubic YSZ thin films and separate them from bulk-limited conductivity.

Results and Discussion

The temperature dependence of the in-plane ionic conductivity was obtained as a function of film thickness over a thickness range of 15 nm to 2 μm for oriented YSZ films grown on MgO (001) substrates. The films were prepared by pulsed laser deposition (PLD) with typical rates of 0.5 to 1 Å per pulse at 5 Hz. The film thickness estimated from these conditions correlates well with value determined from direct observation by electron microscopy. The films exhibited a high degree of epitaxy and a cube-on-cube texture with (002) rocking-curve widths < 1° and in-plane mosaic (111) spreads < 4°. Pole figures obtained of the films revealed a very high degree of (001) texture in the 15 nm thick film, which increases as the film thickness was increased. Observations of cross sections of the 29 and 58 nm films by transmission electron microscopy revealed YSZ films with well-ordered crystalline structures aligned with that of the single-crystal MgO substrate (Fig. 1). In addition, energy-dispersive spectroscopy showed that the yttria content averages~9.5 mol %, and that no discernable impurities are present. Although there were strain contours due to the lattice mismatch between film and substrate (~22% strain), there was little evidence of either extensive dislocation arrays (*e.g.*, subgrain boundaries), within the YSZ film. It should be noted that the large lattice mismatch strains certainly could be a factor in the conductivity results by acting as a driving force for dopant segregation. Future studies will be directed to resolve this problem by employing single crystal substrates with lattice parameters more closely matched to those of the YSZ.

The electrical conductivity was measured by two-probe impedance over a temperature range of 400-800°C in oxygen using silver electrodes. Because YSZ thin films had been deposited on an insulating substrate, the electrode configuration was selected to obtain measurements of the current flow in the plane parallel to the substrate surface. In this case, the total resistance involves the superposition of film, interface, and substrate contributions. However, if the substrate resistance is significantly higher than that of the film and interface, the total resistance will be determined by film and/or film/substrate interface. This electrode arrangement was evaluated by comparing the resistance of the substrate and that of a substrate with a YSZ film. The resultant data showed that the resistance of the
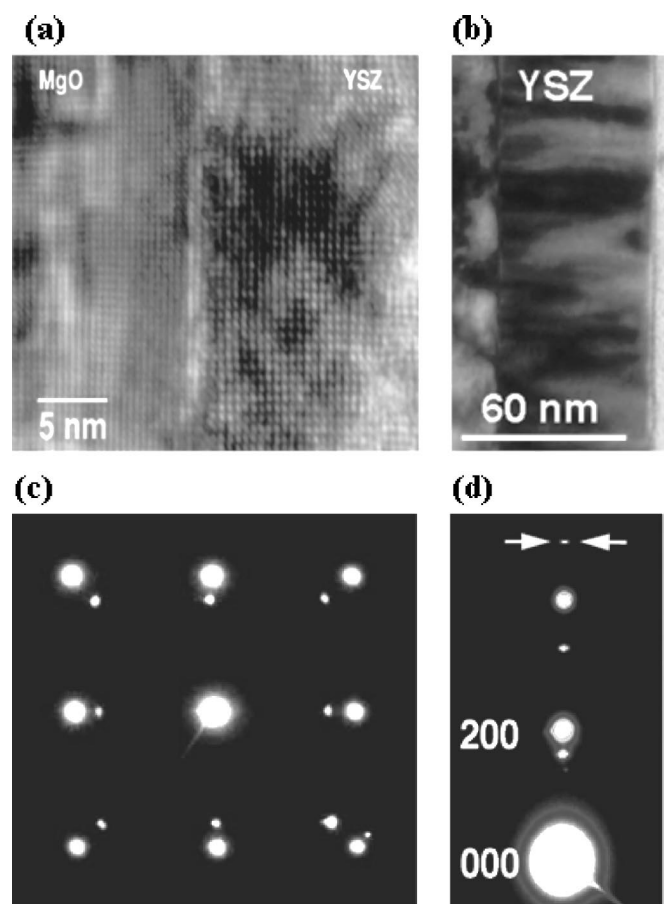
[z] E-mail: kosackiip@ornl.gov

Figure 1. Lattice structure and orientation of YSZ films. (a) The high quality of the YSZ film and the near absence of dislocations are evident in lattice imaging of YSZ film/MgO substrate cross sections. (b) The lattice mismatch between film and substrate results in strain contours. The alignment of the two lattices is evident in the cube-on-cube diffraction pattern in (c) and in the small (≤2°) mosaic spread of the YSZ(001) diffraction spot indicated by arrows in (d).
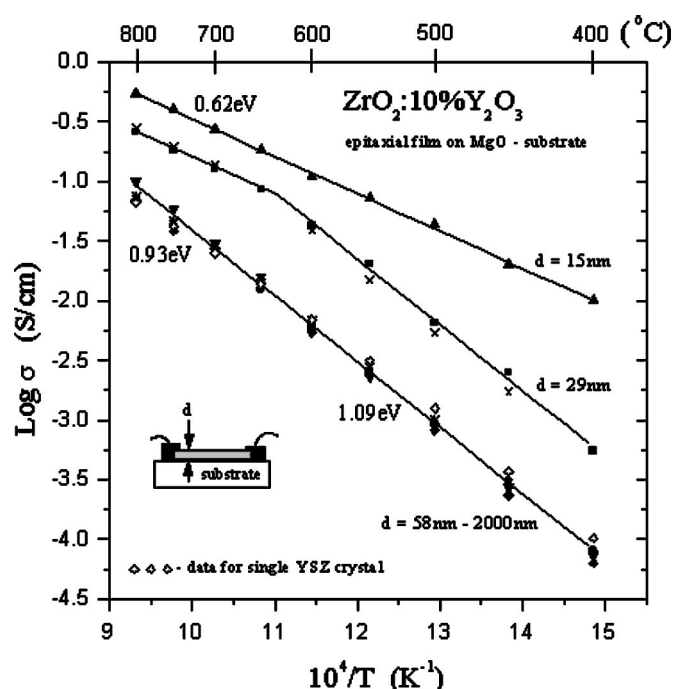

Figure 2. Conductivity measured parallel to the interface of YSZ films. Highly textured YSZ films with thicknesses <30 nm exhibit a substantial increase in conductivity over a temperature range of 400-800°C. The conductivity for the YSZ films remains unaffected for film thicknesses >60 nm and exhibits values that mimic those for both bulk single 9.5 YSZ crystals and microcrystalline YSZ ceramics. Data for YSZ films are shown for the following thicknesses: ▼ 58, ▽ 125, △ 225, and* 565 nm; note that data for 2000 nm thick YSZ film overlaps that for the >60 to ≤565 nm thick films. Data for 29 nm thick YSZ films obtained for increased (×) and decreased (■) temperatures.

substrate is at least two to three orders of magnitude higher than that of the films over the film thickness range studied here (2 μm to 15 nm). This strongly suggests that the influence of the substrate on the conductivity data was negligible. In addition the conductivity measurements were also performed on ZrO_2-9.5 mol % Y_2O_3 bulk single crystals and obtained data were correlated with conductivities of YSZ thin films with thickness ranging from 2 μm to 60 nm. The conductivity activation energies were determined from linear relation of log $\sigma(1/T)$ and are slightly different (about 0.05 eV) than those determined from Arrhenius behavior-log $\sigma T(1/T)$.

As shown in Fig. 2, all the epitaxial films with thicknesses ranging from 58 nm to 2 μm exhibited essentially identical temperature-dependent conductivities and mimicked the response of bulk cubic 9.5 YSZ single crystals. The strong correlation between the conductivity of bulk single crystals and these YSZ films is not surprising in view of the strong cube-on-cube texture of the films. The associated activation energies below 650°C averaged ~1.1 eV for both the single crystals and the thicker epitaxial films. The activation energies decreased somewhat in the higher temperature region (>650°C) and reached values of ~0.9 eV for single crystals and ~1.0 eV for the thicker epitaxial films. The increase in the activation energy was considered to be related to oxygen-vacancy trapping by acceptor impurities, which results in the defect association $(Y'_{Zr} - V_0^{\bullet\bullet})^{\bullet}$ at lower temperatures.[3,16,17]

The conductivity of the 29 nm film is nearly tenfold greater than that of the thicker films below 650°C and threefold above 650°C

(see Fig. 2). An even greater effect is seen for the 15 nm thick film, which exhibits increases in the conductivity of nearly tenfold and 150-fold at 800 and 400°C, respectively. In this case, the activation energy remains ~0.62 eV across the entire temperature range and is lower than the value of 0.9 eV reported for oxygen diffusivity in YSZ single crystal.[17] For the 29 nm film a transition in the activation energies near 650°C is observed. At lower temperatures, the activation energy value is consistent with the activation energy determined for thicker films and single crystals, while above 650°C, the activation energy is comparable to that for 15 nm film. The reversible behavior of the changes in conductivity was observed for both increasing and decreasing temperatures (Fig. 2), this strongly suggests contributions from both bulk and surface/interface attributed processes. The reported changes in the conductivity of YSZ films (Fig. 2) can be associated with either YSZ/MgO interface or to the free surface effects and further studies to separate these contributions are required.

The bulk and surface and/or interface attributed conductivities operate in parallel, and surface/interface contributions increase with decreasing the film thickness, while bulk conductivity should not depend upon thickness. The relationship between the conductivity and film thickness can be interpreted as a superposition of surface/interface and bulk related contributions. The interaction between these are complex and depend on many parameters including material morphology, the volume fraction occupied by the interfacial area, as well as the relaxation time and the activation energy for each transport process. The conductivity of the 29 nm YSZ film illustrates this complexity. The observed behavior is not related to changes in the bulk conductivity but rather to increasing surface/interface contributions with increase in temperatures. In the 15 nm YSZ films, the conductivity is more dominated by surface/interface processes (Fig. 2).
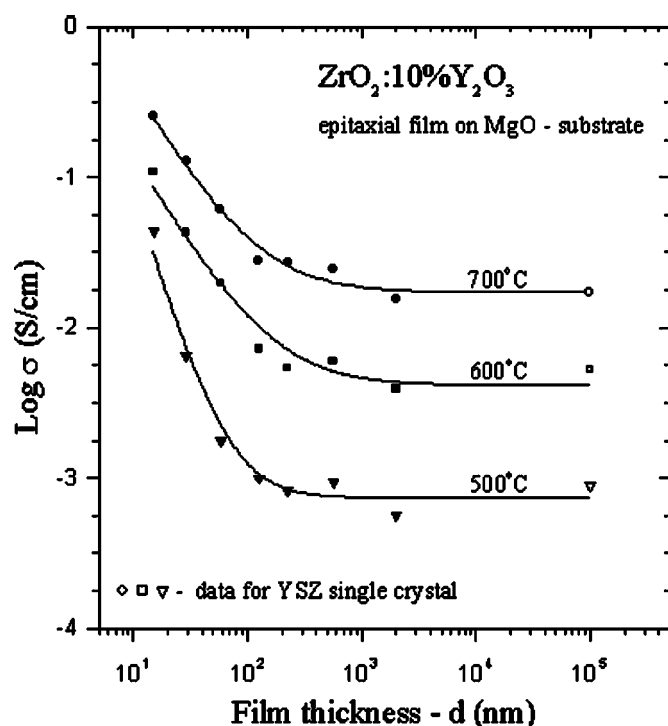
Figure 3. Thickness-dependent conductivity of YSZ films. A dramatic increase in conductivity with decreasing film thickness occurs for films having thicknesses <100 nm, as shown here for selected temperatures in the range of interest. The thickness dependence of the conductivity below 100 nm increases as the temperature decreases and can be correlated with the decrease in the activation energies for these films. For thicknesses >100 nm, where the activation energy is independent of film thickness, the thickness dependence of the conductivity is essentially constant for each temperature.

With the high surface/interfacial area of thin films, there is a potential for water or hydroxyl groups to either degrade the conductivity by defect association or enhance it by protonic conductivity.[18] The potential effects of each was evaluated by annealing a 29 nm thick YSZ film at 800°C for 30 h in a wet atmosphere obtaining by bubbling oxygen trough a column containing 22°C water, which corresponds to a water content of 2.6 wt %. The conductivity determined in wet oxygen is lower than that obtained in dry atmosphere. Also, the activation energy increased from 1.08 to 1.3 eV in dry and wet atmospheres, respectively. This decrease in conductivity can be attributed to the interaction of water with oxygen vacancies and the formation of hydroxyl ions (*i.e.*, $H_2O + V_O^{\cdot\cdot} + O_O^x \rightarrow 2$ OH).[18,19] Because the water itself cannot be introduced into the cubic YSZ lattice,[19] this reaction can only occur on the surface or the interface. The increase in activation energy for the film annealed in wet oxygen is consistent with defect association (*e.g.*, Y'_{Zr}-OH) on the surface.[18] This is consistent with previously published data, which showed that even long (six months) annealing times in a water vapor atmosphere did not influence the bulk conductivity in cubic YSZ.[19] Thus, enhanced protonic conductivity is not a factor in the enhanced conductivity observed for the thinner YSZ (<60 nm) films.

The effect of film thickness on the electrical conductivity at selected temperatures is highlighted in Fig. 3. Here one observes distinct inflections in the conductivity-thickness response for film thickness less than 60 nm where the conductivity rises rapidly with decreasing film thickness and apparently is not saturated in the 15 nm film. This transition in the thickness-dependent conductivity coincides with the shift from a constant activation energy for film thickness >60 nm to one that changes with temperature as the thick-

ness is reduced (Fig. 2). These observations clearly show that ionic conductivity of YSZ can exhibit a substantial nanoscale effect when the film thickness is reduced to below 60 nm. As can be seen in Fig. 3, the overall conductivity of YSZ thin films is determined by the bulk contribution when the film is thicker than 60 nm. However for film thicknesses less than 60 nm, the interface/surface contribution begins to dominate the conductivity. The modeling of the conductivity observed in YSZ films as a function of their thickness and temperature is under study. The obtained preliminary results show that such conductivity behavior can be described using a mixing rules model.[20]

Conclusions

The electrical conductivity of the highly textured cubic YSZ thin films deposited on MgO substrate as a function of temperature and thickness have been evaluated. An increase in the conductivity was observed for films less than 60 nm thick. The highest conductivity of 0.6 S/cm was observed at 800°C for 15 nm thick film. This effect appears to represent an increased contribution of the MgO/YSZ interfacial conductivity with decreasing film thickness. Presented results show that the film thickness can be a scaling factor to enhance the surface phenomena. The similarity in the activation energy for the conductivity of the 15 nm YSZ film and that reported for oxygen surface exchange supported this interpretation. The increase of the conductivity of epitaxial YSZ thin films offers new opportunity for oxygen conductors whose properties can be effectively controlled by tailoring the thickness and lattice mismatch of these nanoscale films.

References

1. *Advances in Ceramics*, Vol. 3, A. H. Heuer and L. W. Hobs, Editors, The American Ceramics Society, Columbus, OH (1981).
2. E. C. Subbarao, *Advances in Ceramics*, Vol. 3, A. H. Heuer and L. W. Hobs, Editors, p. 1, The American Ceramics Society, Columbus, OH (1981).
3. J. F. Baumard and P. Abelard, *Advances in Ceramics*, Vol. 12, N. Clausen, M. Ruhle, and A. H. Heuer, Editors, p. 555, The American Ceramics Society, Columbus, OH (1983).
4. I. Kosacki and H. U. Anderson, in *Ionic and Mixed Conducting Ceramics IV*, T. A. Ramanarayanan, W. L. Worrell, and M. Mogensen, Editors, PV 2001-28, p. 238, The Electrochemical Society Proceedings Series, Pennington, NJ (2001).
5. I. Kosacki and H. U. Anderson, in *Encyclopedia of Materials: Science and Technology*, Vol. 4, p. 3609, Elsevier Science Ltd., New York (2001).
6. T. Suzuki, I. Kosacki, H. U. Anderson, and Ph. Colomban, *J. Am. Ceram. Soc.,* **84**, 2007 (2001).
7. I. Kosacki, H. U. Anderson, Y. Mizutani, and K. Ukai, *Solid State Ionics,* **152-153**, 431 (2002).
8. I. Kosacki, T. Suzuki, V. Petrovsky, and H. U. Anderson, *Solid State Ionics,* **136-137**, 1225 (2000).
9. P. Mondal, A. Klein, W. Jaegermann, and H. Hahn, *Solid State Ionics,* **118**, 331 (1999).
10. M. Aoki, Y.-M. Chiang, I. Kosacki, J.-R. Lee, H. L. Tuller, and Y. J. Liu, *J. Am. Ceram. Soc.,* **79**, 1169 (1996).
11. J. Maier, *Solid State Ionics,* **131**, 13 (2000).
12. K. Otsuka, A. Kuwabara, A. Nakamura, T. Yamamoto, K. Matsunga, and Y. Ikuhara, *Appl. Phys. Lett.,* **82**, 877 (2003).
13. X. Tang, K. P. D. Lagerlof, and A. H. Heuer, *J. Am. Ceram. Soc.,* In press.
14. W. Puin, S. Rodewald, R. Ramlau, P. Heitjans, and J. Maier, *Solid State Ionics,* **131**, 159 (2000).
15. N. Sata, K. Eberman, K. Eberl, and J. Maier, *Nature (London),* **408**, 946 (2000).
16. I. Kosacki, V. Petrovsky, and H. U. Anderson, *J. Electroceram.,* **4**, 243 (2000).
17. P. S. Manning, J. D. Sirman, R. A. De Souza, and J. A. Kilner, *Solid State Ionics,* **100**, 1 (1997).
18. S. Raz, K. Sasaki, J. Maier, and I. Riess, *Solid State Ionics,* **143**, 181 (2001).
19. X. Guo and J. Maier, *J. Electrochem. Soc.,* **148**, E121 (2001).
20. I. Kosacki, Ch. M. Rouleau, P. F. Becher, and D. H. Lowndes, In preparation.